**Novel antiviral activity of PAD inhibitors against human beta-coronaviruses HCoV-OC43 and SARS-CoV-2**

**Novel antiviral activity of PAD inhibitors against human beta-coronaviruses HCoV-OC43 and SARS-CoV-2**

Selina Pasquero[a], Francesca Gugliesi[a], Gloria Griffante[b], Valentina Dell'Oste[a], Matteo Biolatti[a], Camilla Albano[a], Greta Bajetto[a], Serena Delbue[d], Lucia Signorini[d], Maria Dolci[d], Santo Landolfo[a], Marco De Andrea[a,c]

[a] *Department of Public Health and Pediatric Sciences, University of Turin – Medical School, Turin, Italy*
[b] *Department of Translational Medicine, University of Piemonte Orientale, Novara, Italy*
[c] *CAAD Center for Translational Research on Autoimmune and Allergic Disease, University of Piemonte Orientale, Novara Medical School, Italy*
[d] *Department of Biomedical, Surgical and Dental Sciences, University of Milan, Milan, Italy*

**ABSTRACT**

The current SARS-CoV-2 pandemic, along with the likelihood that new coronavirus strains will appear in the nearby future, highlights the urgent need to develop new effective antiviral agents. In this scenario, emerging host-targeting antivirals (HTAs), which act on host-cell factors essential for viral replication, are a promising class of antiviral compounds. Herein, we report the discovery of a new class of HTAs endowed with a potent inhibitory activity against human beta-coronaviruses (HCoVs). Specifically, we show that infection of lung and kidney epithelial cell lines with HCoV-OC43 and SARS-CoV-2 leads to aberrant citrullination of cellular proteins, a posttranslational modification associated with various inflammatory conditions. Most importantly, we show that targeting the cellular enzymes catalyzing protein citrullination—*i.e.*, peptidylarginine deiminases (PADs)—significantly reduces HCoV-OC43 and SARS-CoV-2 replication *in vitro*. Overall, our results demonstrate the potential efficacy of PAD inhibitors in suppressing HCoV infection, which may provide the rationale for the repurposing of this class of inhibitors for the treatment of COVID-19 patients.

## 1. Introduction

In recent years, emerging zoonotic RNA viruses have raised serious public health concerns worldwide. Among them, novel coronaviruses (CoVs) deserve special attention due to their high spillover potential and transmissibility rate, often leading to deadly epidemics across multiple countries, worsened by the lack of effective therapies (Fan et al., 2019).

The *Coronaviridae* family consists of enveloped single-stranded, positive-sense RNA viruses classified into four coronavirus genera: alpha, beta, gamma, and delta. To date, seven human coronaviruses (HCoVs), belonging to the alpha and beta genera, have been identified (Su et al., 2016). HCoV-229E and HCoV-OC43 were first described in 1966 and 1967, respectively, followed by HCoV-NL63 in 2004 and HCoV-HKU1 in 2005. HCoVs generally establish infections in the upper respiratory district—responsible for about 10-30% of common cold cases—, but in vulnerable patients they can also cause bronchiolitis and pneumonia (Leao et al., 2020; Paules et al., 2020).

Even though HCoVs have long been recognized as human pathogens, effective treatments against these viruses have only started to be developed after the severe acute respiratory syndrome CoV (SARS-CoV) outbreak in 2002 (Ksiazek et al., 2003; Weiss and Navas-Martin, 2005). Since then, recurrent spillover events from wildlife have led to the appearance of two other highly pathogenic beta-CoV strains associated with severe respiratory diseases in humans: the Middle East respiratory syndrome coronavirus (MERS-CoV) in 2011, which causes MERS (De Wit et al., 2016; Zaki et al., 2012), and the severe acute respiratory syndrome CoV-2 (SARS-CoV-2) in 2019, the etiological agent of the ongoing pandemic of coronavirus disease 2019 (COVID-19) (Lu et al., 2020; Wu et al., 2020).

In this scenario, the widespread vaccine hesitancy, the growing number of breakthroughs among the vaccinated population, the emergence of increasingly infectious SARS-CoV-2 variants, and the likelihood that new CoV strains will continue to appear in the future have all led to the urgent need to develop new antiviral agents able to tackle ongoing SARS-CoV-2 outbreaks. Consistent with this emergency status, HCoV-OC43 has often been used as a surrogate of—or together with—SARS-

CoV-2 to test potential inhibitors of HCoV replication in both cell-based assays and *in silico* analysis (Milani et al., 2021)

Most of the approved antiviral drugs are the so-called direct-acting antiviral agents (DAAs), compounds designed against viral proteins deemed essential for infection. For example, remdesivir, whose efficacy against SARS-CoV-2 is highly controversial (Hsu, 2020), and molnupiravir, a new oral antiviral highly effective in preventing severe disease based on the results of a recent Phase 2a trial (Fischer et al., 2021), are nucleoside analogue prodrugs acting as competitive substrates for virally-encoded RNA-dependent RNA polymerase (RdRp) (Beigel et al., 2020; Warren et al., 2016). Another emerging class of antiviral agents named host-targeting antivirals (HTAs) consists of drugs acting on host-cell factors involved in viral replication. To date, most studies have focused on the analysis of viral proteins and the identification of potential DAAs. However, viruses encode a limited number of proteins, and those suitable as drug targets are only a subset of them. Therefore, targeted disruption of the mechanisms devised by HCoVs to manipulate the host cellular environment during infection, such as those leading to immune evasion and host gene expression alterations (Hartenian et al., 2020), holds great promise for the treatment of COVID-19 patients.

Peptidyl-arginine deiminases (PADs) are a family of calcium-dependent enzymes that catalyze a posttranslational modification (PTM) named citrullination, also known as deimination, a process during which the guanidinium group of a peptidyl-arginine is hydrolyzed to form peptidyl-citrulline, an unnatural amino acid (Mondal and Thompson, 2019; Witalisom et al., 2002). Five PAD isozymes (PAD 1-4 and 6) are expressed in humans, with a unique distribution in various tissues (Vossenaar et al., 2003). PAD dysregulation leads to aberrant citrullination, which is a typical biomarker of various inflammatory conditions, suggesting that it may play a pathogenic role in inflammation-related diseases (Acharya et al., 2012; Knight et al., 2015; Sokolove et al., 2013; van Venrooij et al., 2011; Yang et al., 2016; Yuzhalin, 2019).

In this scenario, a correlation between PAD dysregulation and viral infections has recently emerged. In particular, the antiviral activity of the LL37 protein appears to be compromised upon

human rhinovirus (HRV)-induced citrullination (Casanova et al., 2020), and sera from RA patients can specifically recognize artificially citrullinated Epstein-Barr virus (EBV) proteins (Pratesi et al., 2011, 2006; Trier et al., 2018). Consistently, we have recently shown that human cytomegalovirus (HCMV) induces PAD-mediated citrullination of several cellular proteins endowed of antiviral activity, including the two IFN-stimulated genes (ISGs) *IFIT1* and *Mx1*, and that the inhibition of this process by the PAD inhibitor Cl-amidine blocks viral replication (Griffante et al., 2021). Finally, another recent study has shown that SARS-CoV-2 infection can modulate PADI gene expression, particularly in lung tissues, leading to the intriguing possibility that PAD enzymes may play a critical role in COVID-19 disease (Arisan et al., 2020).

Based on this evidence, the aim of this work was to ascertain whether PAD inhibitors might constitute a new class of HTAs against HCoVs. For this purpose, we performed cell based-assays to measure the antiviral activity of various well-characterized PAD inhibitors against two members of the beta-CoV genus: HCoV-OC43, the first one to have been discovered, and SARS-CoV-2, the last one to have emerged so far.

Overall, our results show that both HCoV-OC43 and SARS-CoV-2 infections are significantly associated with PAD-mediated citrullination *in vitro*. Importantly, pharmacological inhibition of PAD enzymes inhibits SARS-CoV-2 replication, suggesting that PAD inhibitors may be repurposed to treat COVID-19.

## 2. Materials and methods

### *2.1 Cell lines and viruses*

Human lung fibroblast MRC-5 cells (ATCC® CCL-171) and African green monkey kidney Vero-E6 cells (ATCC®-1586) were propagated in Dulbecco's Modified Eagle Medium (DMEM; Sigma) supplemented with 1% (v/v) penicillin/streptomycin solution (Euroclone) and heat-inactivated 10% (v/v) fetal bovine serum (FBS) (Sigma). The human coronavirus strain OC43

(HCoV-OC43) (ATCC® VR-1558) was kindly provided by Dr. David Lembo (Department of Clinical and Biological Sciences, University of Turin, Turin, Italy). HCoV-OC43 was propagated on MRC-5 cells at 33°C in a humidified 5% $CO_2$ incubator and titrated by standard plaque method on MRC-5 cells, as described elsewhere (Marcello et al., 2020). SARS-CoV-2 was isolated from a nasal-pharyngeal swab positive for SARS-CoV-2. The complete nucleotide sequence of the SARS-CoV-2 isolated strain was deposited at GenBank, at NCBI and at GISAID (accession number: GenBank: MT748758.1; GISAID EPI_ISL 584051).

*2.2 Reagents and treatments*

The PAD inhibitors Cl-amidine (Cl-A), BB-Cl-amidine (BB-Cl), GSK199, and AFM30a—also known as CAY10723—were from Cayman Chemical (Ann Arbor). The compounds were incubated with cells for 1 h prior to infection and kept throughout the whole experiment.

*2.3 Cell viability assay*

MRC-5 or Vero-E6 cells were seeded at a density of $3*10^4$/well in a 96-well plate. After 24 h, cells were treated with different dilutions of the indicated compound or mock-treated using the vehicle alone (DMSO). Seventy-two h after treatment, cell viability was determined using the 3-(4,5-dimethylthiazol-2-yl)-2,5-diphenyltetrazolium bromide (MTT, Sigma) method previously described (Griffante et al., 2021).

*2.4 In vitro antiviral assay*

MRC-5 and Vero-E6 cells were cultured in a 24-well plate for 1 day and then incubated with the aforementioned PAD inhibitors at the indicated concentrations for 1 h. Subsequently, cells were infected with HCoV-OC43 at a multiplicity of infection (MOI) of 0.1. Following virus adsorption (2

h at 33°C), the viral inoculum was removed, and the cell cultures were maintained in medium containing the indicated treatment for 72 h. DMSO was used as negative control. The extent of HCoV-OC43 replication in MRC-5 cells was assessed by titrating the infectivity of supernatants using plaque assay and comparative real-time PCR. For Vero-E6 cells, the extent of HCoV-OC43 replication was assessed by titrating the infectivity of supernatants using comparative real-time PCR.

SARS-CoV-2 *in vitro* infection of Vero-E6 cells and the anti-viral inhibition assay was conducted as described previously (Parisi OI et al., 2021).

*2.5 Plaque assay*

MRC-5 cells were inoculated with 10-fold serial dilutions of the HCoV-OC43. Twenty-four h later, cells were fixed with cold acetone-methanol (50:50) and subjected to indirect immunostaining with an anti-NP-HCoV-OC43 monoclonal antibody (Millipore MAB9012). To determine the virus titer, the number of immunostained foci was counted on each well using the following formula: virus titer (PFU/ml) = number of plaques * 0.1 ml/dilution fold. SARS-CoV-2 plaque assay were performed on VERO-E6 cells as described previously (Parisi OI et al., 2021).

*2.6 Comparative real-time PCR (viral load)*

All molecular analyses were performed according to Milewska *et al*. (Milewska et al., 2016). Briefly, viral nucleic acids were isolated from 200 µl of sample using the TRI Reagent solution (Sigma-Aldrich), according to the manufacturer's instructions. Extracted viral RNA (4 µl per sample) was retrotranscribed and amplified in a 20 µl reaction mixture containing Sensi Fast Probe No Rox One step kit (Bioline) using a CFX Touch Real Time PCR Detection System (BioRad). The primers and probe for N gene amplification (Eurofins) are reported below:

HCoV-OC43 Fw: AGCAACCAGGCTGATGTCAATACC;

HCoV-OC43 Rv: AGCAGACCTTCCTGAGCCTTCAAT;

Probe (HCoV-OC43P_rt): TGACATTGTCGATCGGGACCCAAGTA (5' FAM and 3'TAMRA labeled).

The reaction conditions were as follows: 10 min at 45°C and 20 min at 95°C, followed by 40 cycles of 5 sec at 95°C and 1 min at 60°C.

Quantification of SARS-CoV-2 copy numbers in cell supernatants was evaluated *via* specific qRT-PCR of the *N1* gene, according to the protocols "Coronavirus disease (COVID-19) technical guidance: Laboratory testing for 2019-nCoV in humans" (WHO, 2020) and "CDC 2019-Novel Coronavirus (2019-nCoV) Real-Time RT-PCR Diagnostic Panel" (CDC, 2020), available at: https://www.who.int/emergencies/diseases/novel-coronavirus-2019/technical-guidance/laboratory-guidance and https://www.fda.gov/media/134922/download [last access 25 October 2021]), respectively.

*2.7 Cell-associated RNA isolation and quantitative nucleic acid analysis*

Total RNA was extracted using the TRI Reagent solution (Sigma-Aldrich), and 1 μg of it retrotranscribed using the RevertAid H-Minus FirstStrand cDNA Synthesis Kit (Thermo Fisher Scientific) according to the manufacturer's instructions. Comparison of mRNA expression between treated and untreated samples was performed by SYBR green-based RT-qPCR by Mx3000P apparatus (Santa Clara), using the primers reported previously. As cellular reference, we amplified the housekeeping gene glyceraldehyde-3-phosphate dehydrogenase (GADPH) with the following primers: GAPDH Fw: AGTGGGTGTCGCTGTTGAAGT; GADPH Rv: AACGTGTCAGTGGTGGACCTG. The reaction conditions were as follows: 2 min at 95°C, followed by 40 cycles of 5 sec at 95°C and 1 min at 60°C.

*2.8 Western blot analysis*

MRC-5 or Vero-E6 cells were treated with the indicated compound or equal volumes of DMSO solvent 1 h before infection and throughout the entire duration of the infection. Cells were infected with either HCoV-OC43 or SARS-CoV-2 at an MOI of 1. Cells were harvested at the indicated time, and lysates were prepared and subjected to Western blot analysis. The primary antibodies were as follows: anti-HCoV-OC43 (Millipore MAB9012); anti-PAD1 (ABCAM); anti-PAD2 (Cosmo Bio); anti-PAD3 (ABCAM); anti-PAD4 (ABCAM); anti-PAD6 (ABCAM); anti-ACTIN (Sigma Aldrich), anti-SARS-CoV-2 (GeneTex).

*2.9 Detection of citrullination with rhodamine-phenylglyoxal (Rh-PG)*

Whole-cell protein extracts were prepared and subjected to immunoblotting as previously described. Equal amounts of protein were diluted with trichloroacetic acid and incubated with rhodamine phenylglyoxal (Rh-PG, Cayman) probe as described in (Griffante et al., 2021).

*2.10 Statistical analysis*

All data were analyzed using GraphPad Prism (GraphPad Software, San Diego, CA). All results are presented as means ± SEM. The half-maximal inhibitory concentrations ($IC_{50}$) and half-maximal cytotoxic concentration ($CC_{50}$) values were calculated by Quest Graph™ IC50 Calculator (AAT Bioquest, Inc, https://www.aatbio.com/tools/ic50-calculator). The selectivity index (SI) values were calculated as the ratio of $CC_{50}$ and $IC_{50}$ (SI= $CC_{50}$/ $IC_{50}$). The *P*-value was calculated by comparing between % inhibition of infected-treated samples and % inhibition of infected-untreated samples. One-tailed Student's t-test was used to compare groups. Significance was considered statistically significant at a *P*-value < 0.05 (*), < 0.01 (**), < 0.001 (***) and < 0.0001 (****).

## 3. Results

*3.1. PAD inhibition blocks HCoV-OC43 replication in MRC-5 cells*

We previously demonstrated that HCMV triggers PAD-mediated citrullination to promote its replication (Griffante et al., 2021). To evaluate whether the protein citrullination profile would also be altered during HCoV infection, we first performed an electrophoresis analysis of protein lysates obtained from MRC-5 lung fibroblasts infected with HCoV-OC43 (MOI 1) incubated with the citrulline-specific probe Rh-PG. At 48 and 72 h post infection (hpi), HCoV-OC43-infected MRC5 cells, but not mock-infected cells, showed a robust increase in total protein citrullination (Fig. 1A). Of note, the expression of viral nucleoprotein (OC43 NP) was only detected in HCoV-OC43-infected MRC5 cells, confirming the successful infection of these cells (Fig. 1A).

Next, to test whether PAD enzymatic activity plays a functional role in HCoV-OC43 replication, we treated infected cells with the two pan-PAD inhibitors Cl-A and BB-Cl and assessed viral RNA synthesis by RT-PCR. Incubation of HCoV-OC43-infected MRC5 cells with increasing amounts of the inhibitors led to a dose-dependent reduction of viral genome copies, a drop that became statistically significant at 50 μM for Cl-A and 0.5 μM for BB-Cl (Fig. 1B and 1C). The calculated $IC_{50}$ for Cl-A and BB-Cl were 34.76 μM and 0.54 μM, respectively. To rule out compound cytotoxicity, HCoV-OC43-infected MRC-5 cells were subjected to MTT assay. The results shown in Fig. S1A, B demonstrate that none of the PAD inhibitors significantly reduced cell viability at the two aforementioned $IC_{50}$. Table 1 shows the $CC_{50}$ for Cl-A (949.14 μM) and BB-Cl (10.12 μM). Based on the calculated $IC_{50}$ and $CC_{50}$, the SIs of Cl-A and BB-Cl in HCoV-OC43-infected MRC-5 were quite similar and both greater than 10 (27.3 and 18.6, respectively). Consistent with the results obtained measuring viral RNA, Cl-A and BB-Cl drastically reduced both intra- and extra-cellular viral genome copy numbers (Fig. 1D), confirming the key role of citrullination in HCoV-OC43 replication and viral cycle.

To determine whether PAD inhibition would prevent viral replication and/or the production of infectious viral particles, we assessed HCoV-OC43 NP expression by Western blotting and the virus yield by plaque assay using the cell extracts and supernatants of HCoV-OC43-infected MRC-5 cells treated with 100 μM Cl-A and 2.5 μM BB-Cl, as previously described. Interestingly, both Cl-A

and BB-Cl treatments significantly reduced HCoV-OC43 NP expression in the very same total protein extracts in which a partial suppression of the citrullination profile was also observed by Rh-PG (Fig. 1E). Moreover, the two drugs significantly reduced PFUs per mL of supernatant by more than 2 and 1 logs, respectively (Fig. 1F).

*3.2. PAD4 plays a central role in HCoV-OC43 replication*

To gain more insight into the mechanism of HCoV-OC43-induced cellular citrullination, we asked which of the five known PAD isoforms (PAD1-4 and PAD6) would be preferentially modulated following HCoV-OC43 infection. To answer this question, we performed immunoblot analysis on whole protein lysates obtained from mock and HCoV-OC43-infected MRC5 cells collected at different time-points after infection (Fig. 2A). PAD2 and PAD4 were the only two PAD isoforms expressed in these cells, with PAD4 being the only one induced upon infection, as judged by densitometry. By contrast, PAD1, 3, and 6 were neither detectable in mock cells nor induced upon infection (Fig. 2A).

Given the above, we next sought to determine whether targeting the enzymatic activity of PAD4 would affect viral replication. To this end, OC43-infected MRC-5 cells were treated with increasing concentrations of the PAD4-specific inhibitor GSK199 or the PAD2-specific inhibitor AFM30a, as negative control, and assessed for their antiviral activity. As expected, AFM30a only partially suppressed the HCoV-OC43 replication rate—never exceeding 40% inhibition within the range of concentrations tested (Fig. 2B). In contrast, GSK199 treatment hampered viral genome production in a dose-dependent manner ($IC_{50}$= 0.6 μM), achieving a complete block of viral replication at 20 μM (Fig. 2C). Furthermore, MRC-5 cells treated with 20 μM GSK199 were viable, ruling out any unspecific effect due to compound toxicity (Fig. S2). Of note, we could only observe significant cytotoxicity of both compounds at concentrations above 100 μM (data not shown). This conferred them an SI > 10, which was particularly robust in the case of GSK199 (224.94) (Table 1).

To confirm these results, we measured the number of viral genome copies in cell lysates and supernatants from MRC-5 cells treated with 20 μM AFM30a or GSK199 and infected with HCoV-OC43. As expected, inhibition of PAD4 by GSK199 drastically reduced the relative viral genome copy number in both compartments compared to vehicle-treated cells, while PAD2 inhibition by AFM30a led to a much less pronounced reduction of viral genome (Fig. 2D). Consistently, immunoblot analysis of total protein extracts from HCoV-OC43-infected MRC-5 cells treated with GSK199 showed a dramatic downregulation of OC43 NP protein expression levels in comparison with vehicle-treated infected cells (Fig. 2E). In contrast, treatment with the PAD2 inhibitor AFM30a only led to a slight decrease in NP protein levels. Fittingly, plaque assay on these cells confirmed a significant reduction of the viral titer in the presence of GSK199 (~2-log reduction), while the inhibitory activity of AFM30a at the same concentration was barely detectable (Fig. 2F).

Taken together, these results suggest that PAD4 plays a major role in HCoV-OC43 replication, and that PAD4 inhibitors are promising anti-HCoV compounds.

*3.3. PAD inhibitors affect HCoV-OC43 and SARS-CoV-2 replication in Vero-E6 cells*

Since Vero-E6 cells represent a widely used cellular system to study beta-CoV replication in the presence of candidate antiviral compounds, we sought to extend our results also to this model. Initially, we performed a quantitative analysis of HCoV-OC43 viral RNA production at 72 hpi using different concentrations of Cl-A (50-300 μM) and BB-Cl (5-20 μM). As depicted in Fig. 3, we observed a marked reduction of viral genome replication in Vero-E6 cells treated with either 150-300 μM Cl-A (panel A) or 20 μM BB-Cl (panel B) compared to their vehicle-treated counterparts. These pronounced effects were not a consequence of an intrinsic cytotoxicity of the PAD inhibitors as none of the screened compounds significantly reduced cell viability at the same concentrations as those used in the antiviral assays (Fig. S3A, B and Table 1).

Next, to evaluate whether HCoV-OC43 infection would also trigger protein citrullination in Vero-E6 cells, we performed electrophoresis analysis of protein lysates obtained from cells infected

with HCoV-OC43 using the Rh-PG probe. As shown in Fig. 3C, protein citrullination of HCoV-OC43-infected Vero-E6 cells was significantly induced at 48 hpi, whereas it remained almost unchanged in infected cells treated with 300 μM of the Cl-A inhibitor.

To extend our findings to other beta-CoVs, we examined the impact of PAD inhibitors treatment on SARS-CoV-2 viral genome replication. As shown in Figs. 3D and 3E, both Cl-A and BB-Cl treatments suppressed SARS-CoV-2 viral genome replication in a dose-dependent manner, albeit to a lower extent than that observed for HCoV-OC43.

To characterize the protein citrullination profile during SARS-CoV-2 infection, protein lysates obtained from Vero-E6 cells infected with SARS-CoV-2, treated with or without Cl-A, were analyzed by Rh-PG (Fig. 3F). The citrullination profile of these SARS-CoV-2-infected cells was consistent with that observed upon HCoV-OC43 infection, both displaying a signal lower than 50 kDa, which specifically appeared after the infection. However, unlike what we observed in HCoV-OC43-infected cells, the citrullination signal, albeit strongly reduced, it never completely disappeared following Cl-A treatment. In line with this observation, Cl-A treatment led to ~50% reduction of SARS-CoV-2 NP protein expression (Fig. 3F). To corroborate these results, we carried out plaque reduction assays in SARS-CoV-2-infected Vero-E6 cells treated with 300 μM Cl-A as described above. Consistent with our previous results, the inhibition of PAD catalytic activity resulted in a reduction of 1 log in SARS-CoV-2 yield (Fig. 3G).

Altogether, our results demonstrate that beta-CoV infection is associated with protein citrullination. Moreover, treatment of HCoV-OC43 and SARS-CoV-2-infected cells with PAD pan-inhibitors inhibits virus replication restoring the physiological citrullination profile.

## 4. Discussion

We have recently shown that HCMV infection triggers PAD-mediated citrullination of several host proteins in primary human fibroblasts, and that this activity enhances viral fitness *per se* (Griffante et al., 2021). Here, we extend those findings to two RNA viruses, HCoV-OC43 and SARS-

CoV-2, which we demonstrate to be both capable of promoting PAD-mediated citrullination *in vitro*. In particular, we show that HCoV-OC43 infection of MRC-5 lung fibroblasts upregulates PAD4-mediated citrullination of proteins, and that this process is required for optimal viral replication. A similar induction in citrullination levels was also found in CoV-infected Vero-E6 cells, a non-human model system widely used to study HCoVs, especially SARS-CoV-2 (Dittmar et al., 2021; Ghosh et al., 2021; Milani et al., 2021; Wing et al., 2021), suggesting that HCoVs can modulate citrullination across species.

Citrullination is a posttranslational modification mediated by PAD family members, whose distribution and expression patterns are modulated by inflammatory signals in a tissue-specific manner (Acharya et al., 2012; Knight et al., 2015; Vossenaar et al., 2003; Willis et al., 2011; Yang et al., 2016). Fittingly, we and others have recently reported a positive association between viral infection and PAD-mediated upregulation of citrullination in different cellular models (Arisan et al., 2020; Casanova et al., 2020; Griffante et al., 2021), raising the important question as to whether pharmacological inhibition of PAD activity can be used to reduce viral replication in infected patients. In support of this possibility, we found that treatment of HCMV-infected HFFs with the pan PAD inhibitor Cl-A downregulated PAD2 and 4-mediated citrullination of cellular proteins, thereby blocking viral replication *in vitro* (Griffante et al., 2021). In the present study, we provide additional evidence supporting the use of PAD inhibitors to curb viral growth. Specifically, we show that treatment of HCoV-OC43-infected MRC-5 cells with either of the two pan-PAD inhibitors Cl-A and BB-Cl (Biron et al., 2016; Knight et al., 2015; Ledet et al., 2018; Willis et al., 2011) or the specific PAD4 inhibitor GSK199, but not the PAD2 inhibitor AFM30a, can efficiently inhibit viral replication. This finding is consistent with the fact that MRC-5 cells express basal levels of both PAD2 and PAD4, but only PAD4 is significantly upregulated upon viral infection. Furthermore, the observation that Cl-A or BB-Cl treatment markedly reduces the presence of viral genome copies in both cellular extracts and supernatants indicates that these compounds not only block viral replication but also reduce the production of infectious particles. Of note, the considerable reduction in viral

replication and titer by the GSK199 compound was achieved at concentrations that do not affect cell viability. Indeed, the high SI of GSK199 (224.94, Table 1) along with its potent antiviral activity makes this PAD4 inhibitor an attractive target for further therapeutic development, a possibility further supported by results showing that targeting PAD4 led to a significant improvement of the clinical and histopathological end-points in a preclinical model of murine arthritis (Willis et al., 2017). Another important aspect that supports the repurposing of PAD inhibitors for antiviral therapy is that their efficacy in treating various inflammatory conditions, such as arthritis, colitis, and sepsis, has already been confirmed in preclinical and *in vitro* studies, all showing a good safety profile of such compounds (Chumanevich et al., 2011; Willis et al., 2011; Zhao et al., 2016).

Our results, showing a strong induction of citrullination levels in SARS-CoV-2-infected Vero-E6 cells also highlight the potential use of PAD inhibitors to treat COVID-19 patients. It is in fact conceivable to envisage an association between SARS-CoV-2 infection and aberrant citrullination as a way to induce an inflammatory state in different tissues (Delorey et al., 2021). This would be supported by a recent study by Arisan and co-workers showing that SARS-CoV-2 infection can modulate PADI gene expression in lung tissues (Arisan et al., 2020). In good agreement, here we show that the inhibitory activity of Cl-A and BB-Cl is not only restricted to HCoV-OC43-infected fibroblasts, but it can also be extended to SARS-CoV-2-infected Vero-E6 cells, highly permissive cells commonly used to propagate and study beta-CoV strains (Ogando et al., 2020). In these cells, both compounds efficiently suppress SARS-CoV-2 genome replication in a dose-dependent manner, albeit to higher concentrations than those used to inhibit HCoV-OC43 replication. Further experiments are ongoing to test whether this difference is virus-dependent or cell line-dependent. However, also in this case the concentrations of Cl-A (150-300 μM) or BB-Cl (20 μM) capable of reducing of about 1 log the SARS-CoV-2 yield in Vero-E6 cells were not associated with significant cytotoxic effects. Similar to what seen for HCoV-OC43-infected MRC-5 cells, inhibition of PAD activity counteracted SARS-CoV-2-induced citrullination.

In the current pandemic of COVID-19, it is more important than ever that the most promising anti-SARS-CoV-2 drug candidates enter clinical development. Based on some similarities between the clinical outcome observed in autoimmune/autoinflammatory disease and COVID-19, including lung involvement and aberrant cytokine release, pan- and specific-PAD inhibitors—i.e., GSK199—repurposing can be foreseen as a valuable strategy, as it enables accelerating the use of compounds with already known safety profiles. Moreover, treatments based on molecules with beneficial multi-target activities—a concept known as polypharmacology (Ravikumar and Aittokallio, 2018)—, which may help to counteract multiple complications as those observed in COVID-19 patients, may show an increased antiviral spectrum.

In conclusion, our findings unveil an unprecedented role of citrullination in the replication of the two human coronaviruses HCoV-OC43 and SARS-CoV-2 in lung and kidney epithelial cells. We also provide evidence that increased PAD activity is required for β-HCoV replication, highlighting the potential use of PAD inhibitors as novel HTAs against β-HCoV infections. Experiments are ongoing to test the anti-β-HCoV efficacy and safety of other PAD inhibitors. Moreover, based on the current availability of different animal models to be exploited for SARS-CoV-2 replication (Lee and Lowen, 2021), including K18-hACE2 transgenic mice challenged with SARS-CoV-2 (Conforti et al., 2021), investigations are being performed to test the feasibility of our drug repurposing strategy *in vivo*.

**Acknowledgments**

We thank Marcello Arsura for critically reviewing the manuscript. This research was supported by the University of Turin (PoC - TOINPROVE/2020, RILO2020 and RILO2021 to M.D.A.), by the Ministry of Education, University and Research – MIUR (PRIN Project 2017ALPCM to V.D.O.) and by the AGING Project—Department of Excellence—Department of Translational Medicine, University of Piemonte Orientale (G.G.).

**Bibliography**


Acharya, N.K., Nagele, E.P., Han, M., Coretti, N.J., DeMarshall, C., Kosciuk, M.C., Boulos, P.A., Nagele, R.G., 2012. Neuronal PAD4 expression and protein citrullination: Possible role in production of autoantibodies associated with neurodegenerative disease. Journal of Autoimmunity 38, 369–380. https://doi.org/10.1016/j.jaut.2012.03.004

Arisan, E.D., Uysal-Onganer, P., Lange, S., 2020. Putative roles for peptidylarginine deiminases in COVID-19. International Journal of Molecular Sciences 21, 1–29. https://doi.org/10.3390/ijms21134662

Beigel, J.H., Tomashek, K.M., Dodd, L.E., Mehta, A.K., Zingman, B.S., Kalil, A.C., Hohmann, E., Chu, H.Y., Luetkemeyer, A., Kline, S., Lopez de Castilla, D., Finberg, R.W., Dierberg, K., Tapson, V., Hsieh, L., Patterson, T.F., Paredes, R., Sweeney, D.A., Short, W.R., Touloumi, G., Lye, D.C., Ohmagari, N., Oh, M., Ruiz-Palacios, G.M., Benfield, T., Fätkenheuer, G., Kortepeter, M.G., Atmar, R.L., Creech, C.B., Lundgren, J., Babiker, A.G., Pett, S., Neaton, J.D., Burgess, T.H., Bonnett, T., Green, M., Makowski, M., Osinusi, A., Nayak, S., Lane, H.C., 2020. Remdesivir for the Treatment of Covid-19 — Final Report. New England Journal of Medicine 383, 1813–1826. https://doi.org/10.1056/nejmoa2007764

Biron, B.M., Chung, C.-S., O'brien, X.M., Chen, Y., Reichner, J.S., Ayala, A., 2016. E-Mail Cl-Amidine Prevents Histone 3 Citrullination and Neutrophil Extracellular Trap Formation, and Improves Survival in a Murine Sepsis Model. https://doi.org/10.1159/000448808

Casanova, V., Sousa, F.H., Shakamuri, P., Svoboda, P., Buch, C., D'Acremont, M., Christophorou, M.A., Pohl, J., Stevens, C., Barlow, P.G., 2020. Citrullination Alters the Antiviral and Immunomodulatory Activities of the Human Cathelicidin LL-37 During Rhinovirus Infection. Frontiers in Immunology 11. https://doi.org/10.3389/fimmu.2020.00085

Chumanevich, A.A., Causey, C.P., Knuckley, B.A., Jones, J.E., Poudyal, D., Chumanevich, A.P., Davis, T., Matesic, L.E., Thompson, P.R., Hofseth, L.J., 2011. Suppression of colitis in mice by Cl-amidine: a novel peptidylarginine deiminase inhibitor. Am J Physiol Gastrointest Liver Physiol 300, G929-938. https://doi.org/10.1152/ajpgi.00435.2010

Conforti, A., Marra, E., Palombo, F., Roscilli, G., Ravà, M., Fumagalli, V., Muzi, A., Maffei, M., Luberto, L., Lione, L., Salvatori, E., Compagnone, M., Pinto, E., Pavoni, E., Bucci, F., Vitagliano, G., Stoppoloni, D., Pacello, M.L., Cappelletti, M., Ferrara, F.F., D'Acunto, E., Chiarini, V., Arriga, R., Nyska, A., Di Lucia, P., Marotta, D., Bono, E., Giustini, L., Sala, E., Perucchini, C., Paterson, J., Ryan, K.A., Challis, A.-R., Matusali, G., Colavita, F., Caselli, G., Criscuolo, E., Clementi, N., Mancini, N., Groß, R., Seidel, A., Wettstein, L., Münch, J., Donnici, L., Conti, M., De Francesco, R., Kuka, M., Ciliberto, G., Castilletti, C., Capobianchi, M.R., Ippolito, G., Guidotti, L.G., Rovati, L., Iannacone, M., Aurisicchio, L., 2021. COVID-eVax, an electroporated DNA vaccine candidate encoding the SARS-CoV-2 RBD, elicits protective responses in animal models. Mol Ther S1525-0016(21)00466–4. https://doi.org/10.1016/j.ymthe.2021.09.011

De Wit, E., Van Doremalen, N., Falzarano, D., Munster, V.J., 2016. SARS and MERS: Recent insights into emerging coronaviruses. Nature Reviews Microbiology. https://doi.org/10.1038/nrmicro.2016.81

Delorey, T.M., Ziegler, C.G.K., Heimberg, G., Normand, R., Yang, Y., Segerstolpe, Å., Abbondanza, D., Fleming, S.J., Subramanian, A., Montoro, D.T., Jagadeesh, K.A., Dey, K.K., Sen, P., Slyper, M., Pita-Juárez, Y.H., Phillips, D., Biermann, J., Bloom-Ackermann, Z., Barkas, N., Ganna, A., Gomez, J., Melms, J.C., Katsyv, I., Normandin, E., Naderi, P., Popov, Y.V., Raju, S.S., Niezen, S., Tsai, L.T.-Y., Siddle, K.J., Sud, M., Tran, V.M., Vellarikkal, S.K., Wang, Y., Amir-Zilberstein, L., Atri, D.S., Beechem, J., Brook, O.R., Chen, J., Divakar, P., Dorceus, P., Engreitz, J.M., Essene, A., Fitzgerald, D.M., Fropf, R., Gazal, S., Gould, J., Grzyb, J., Harvey, T., Hecht, J., Hether, T., Jané-Valbuena, J., Leney-Greene, M., Ma, H., McCabe, C., McLoughlin, D.E., Miller, E.M., Muus, C., Niemi, M., Padera, R., Pan, L., Pant, D., Pe'er, C., Pfiffner-Borges, J., Pinto, C.J., Plaisted, J., Reeves, J., Ross, M., Rudy, M., Rueckert, E.H., Siciliano, M., Sturm, A., Todres, E., Waghray, A., Warren, S., Zhang, S., Zollinger, D.R., Cosimi, L., Gupta, R.M., Hacohen, N., Hibshoosh, H., Hide, W., Price, A.L., Rajagopal, J., Tata, P.R., Riedel, S., Szabo, G., Tickle, T.L., Ellinor, P.T., Hung, D., Sabeti, P.C., Novak, R., Rogers, R., Ingber, D.E., Jiang, Z.G., Juric, D., Babadi, M., Farhi, S.L., Izar, B., Stone, J.R., Vlachos, I.S., Solomon, I.H., Ashenberg, O., Porter, C.B.M., Li, B., Shalek, A.K., Villani, A.-C., Rozenblatt-Rosen, O., Regev, A., 2021. COVID-19 tissue atlases reveal SARS-CoV-2 pathology and cellular targets. Nature 595, 107–113. https://doi.org/10.1038/s41586-021-03570-8

Dittmar, M., Lee, J.S., Whig, K., Segrist, E., Li, M., Kamalia, B., Castellana, L., Ayyanathan, K., Cardenas-Diaz, F.L., Morrisey, E.E., Truitt, R., Yang, W., Jurado, K., Samby, K., Ramage, H., Schultz, D.C., Cherry, S., 2021. Drug repurposing screens reveal cell-type-specific entry pathways and FDA-approved drugs active against SARS-Cov-2. Cell Reports 35, 108959. https://doi.org/10.1016/j.celrep.2021.108959

Fan, Y., Zhao, K., Shi, Z.L., Zhou, P., 2019. Bat coronaviruses in China. Viruses. https://doi.org/10.3390/v11030210

Fischer, W., Eron, J.J., Holman, W., Cohen, M.S., Fang, L., Szewczyk, L.J., Sheahan, T.P., Baric, R., Mollan, K.R., Wolfe, C.R., Duke, E.R., Azizad, M.M., Borroto-Esoda, K., Wohl, D.A., Loftis, A.J., Alabanza, P., Lipansky, F., Painter, W.P., 2021. Molnupiravir, an Oral Antiviral Treatment for COVID-19. https://doi.org/10.1101/2021.06.17.21258639

Ghosh, A.K., Miller, H., Knox, K., Kundu, M., Henrickson, K.J., Arav-Boger, R., 2021. Inhibition of Human Coronaviruses by Antimalarial Peroxides. ACS Infectious Diseases. https://doi.org/10.1021/acsinfecdis.1c00053

Griffante, G., Gugliesi, F., Pasquero, S., Dell'Oste, V., Biolatti, M., Salinger, A.J., Mondal, S., Thompson, P.R., Weerapana, E., Lebbink, R.J., Soppe, J.A., Stamminger, T., Girault, V., Pichlmair, A., Oroszlán, G., Coen, D.M., De Andrea, M., Landolfo, S., 2021. Human cytomegalovirus-induced host protein citrullination is crucial for viral replication. Nature Communications 12, 1–14. https://doi.org/10.1038/s41467-021-24178-6

Hartenian, E., Nandakumar, D., Lari, A., Ly, M., Tucker, J.M., Glaunsinger, B.A., 2020. The molecular virology of coronaviruses. Journal of Biological Chemistry 295, 12910–12934. https://doi.org/10.1074/jbc.REV120.013930

Hsu, J., 2020. Covid-19: What now for remdesivir? BMJ 371, m4457. https://doi.org/10.1136/bmj.m4457

Knight, J.S., Subramanian, V., O'Dell, A.A., Yalavarthi, S., Zhao, W., Smith, C.K., Hodgin, J.B., Thompson, P.R., Kaplan, M.J., 2015. Peptidylarginine deiminase inhibition disrupts NET

formation and protects against kidney, skin and vascular disease in lupus-prone MRL/ *lpr* mice. Annals of the Rheumatic Diseases 74, 2199–2206. https://doi.org/10.1136/annrheumdis-2014-205365

Ksiazek, T.G., Erdman, D., Goldsmith, C.S., Zaki, S.R., Peret, T., Emery, S., Tong, S., Urbani, C., Comer, J.A., Lim, W., Rollin, P.E., Dowell, S.F., Ling, A.-E., Humphrey, C.D., Shieh, W.-J., Guarner, J., Paddock, C.D., Rota, P., Fields, B., DeRisi, J., Yang, J.-Y., Cox, N., Hughes, J.M., LeDuc, J.W., Bellini, W.J., Anderson, L.J., 2003. A Novel Coronavirus Associated with Severe Acute Respiratory Syndrome. New England Journal of Medicine 348, 1953–1966. https://doi.org/10.1056/nejmoa030781

Leao, J.C., Gusmao, T.P. de L., Zarzar, A.M., Leao Filho, J.C., Barkokebas Santos de Faria, A., Morais Silva, I.H., Gueiros, L.A.M., Robinson, N.A., Porter, S., Carvalho, A. de A.T., 2020. Coronaviridae—Old friends, new enemy! Oral Diseases 0–3. https://doi.org/10.1111/odi.13447

Ledet, M.M., Anderson, R., Harman, R., Muth, A., Thompson, P.R., Coonrod, S.A., Van de Walle, G.R., 2018. BB-Cl-Amidine as a novel therapeutic for canine and feline mammary cancer via activation of the endoplasmic reticulum stress pathway. BMC Cancer 18, 1–13. https://doi.org/10.1186/s12885-018-4323-8

Lee, C.-Y., Lowen, A.C., 2021. Animal models for SARS-CoV-2. Current Opinion in Virology 48, 73–81. https://doi.org/10.1016/j.coviro.2021.03.009

Lu, R., Zhao, X., Li, J., Niu, P., Yang, B., Wu, H., Wang, W., Song, H., Huang, B., Zhu, N., Bi, Y., Ma, X., Zhan, F., Wang, L., Hu, T., Zhou, H., Hu, Z., Zhou, W., Zhao, L., Chen, J., Meng, Y., Wang, J., Lin, Y., Yuan, J., Xie, Z., Ma, J., Liu, W.J., Wang, D., Xu, W., Holmes, E.C., Gao, G.F., Wu, G., Chen, W., Shi, W., Tan, W., 2020. Genomic characterisation and epidemiology of 2019 novel coronavirus: implications for virus origins and receptor binding. The Lancet 395, 565–574. https://doi.org/10.1016/S0140-6736(20)30251-8

Marcello, A., Civra, A., Milan Bonotto, R., Nascimento Alves, L., Rajasekharan, S., Giacobone, C., Caccia, C., Cavalli, R., Adami, M., Brambilla, P., Lembo, D., Poli, G., Leoni, V., 2020. The cholesterol metabolite 27-hydroxycholesterol inhibits SARS-CoV-2 and is markedly decreased in COVID-19 patients. Redox Biology 36, 101682. https://doi.org/10.1016/j.redox.2020.101682

Milani, M., Donalisio, M., Bonotto, R.M., Schneider, E., Arduino, I., Boni, F., Lembo, D., Marcello, A., Mastrangelo, E., 2021. Combined in silico and in vitro approaches identified the antipsychotic drug lurasidone and the antiviral drug elbasvir as SARS-CoV2 and HCoV-OC43 inhibitors. Antiviral Research 189, 105055. https://doi.org/10.1016/j.antiviral.2021.105055

Milewska, A., Kaminski, K., Ciejka, J., Kosowicz, K., Zeglen, S., Wojarski, J., Nowakowska, M., Szczubiałka, K., Pyrc, K., 2016. HTCC: Broad range inhibitor of coronavirus entry. PLoS ONE 11, 1–17. https://doi.org/10.1371/journal.pone.0156552

Mondal, S., Thompson, P.R., 2019. Protein Arginine Deiminases (PADs): Biochemistry and Chemical Biology of Protein Citrullination. Accounts of Chemical Research 52, 818–832. https://doi.org/10.1021/acs.accounts.9b00024

Ogando, N.S., Dalebout, T.J., Zevenhoven-Dobbe, J.C., Limpens, R.W.A.L., van der Meer, Y., Caly, L., Druce, J., de Vries, J.J.C., Kikkert, M., Bárcena, M., Sidorov, I., Snijder, E.J., 2020. SARS-coronavirus-2 replication in Vero E6 cells: replication kinetics, rapid adaptation and cytopathology. J Gen Virol 101, 925–940. https://doi.org/10.1099/jgv.0.001453

Paules, C.I., Marston, H.D., Fauci, A.S., 2020. Coronavirus Infections-More Than Just the Common Cold. JAMA - Journal of the American Medical Association. https://doi.org/10.1001/jama.2020.0757

Pratesi, F., Tommasi, C., Anzilotti, C., Chimenti, D., Migliorini, P., 2006. Deiminated Epstein-Barr virus nuclear antigen 1 is a target of anti-citrullinated protein antibodies in rheumatoid arthritis. Arthritis and Rheumatism 54, 733–741. https://doi.org/10.1002/art.21629

Pratesi, F., Tommasi, C., Anzilotti, C., Puxeddu, I., Sardano, E., Di Colo, G., Migliorini, P., 2011. Antibodies to a new viral citrullinated peptide, VCP2: fine specificity and correlation with anti-cyclic citrullinated peptide (CCP) and anti-VCP1 antibodies. Clinical & Experimental Immunology 164, 337–345. https://doi.org/10.1111/j.1365-2249.2011.04378.x

Ravikumar, B., Aittokallio, T., 2018. Improving the efficacy-safety balance of polypharmacology in multi-target drug discovery. Expert Opin Drug Discov 13, 179–192. https://doi.org/10.1080/17460441.2018.1413089

Sokolove, J., Brennan, M.J., Sharpe, O., Lahey, L.J., Kao, A.H., Krishnan, E., Edmundowicz, D., Lepus, C.M., Wasko, M.C., Robinson, W.H., 2013. Brief report: citrullination within the atherosclerotic plaque: a potential target for the anti-citrullinated protein antibody response in rheumatoid arthritis. Arthritis Rheum 65, 1719–1724. https://doi.org/10.1002/art.37961

Su, S., Wong, G., Shi, W., Liu, J., Lai, A.C.K., Zhou, J., Liu, W., Bi, Y., Gao, G.F., 2016. Epidemiology, Genetic Recombination, and Pathogenesis of Coronaviruses. https://doi.org/10.1016/j.tim.2016.03.003

Trier, N.H., Holm, B.E., Heiden, J., Slot, O., Locht, H., Lindegaard, H., Svendsen, A., Nielsen, C.T., Jacobsen, S., Theander, E., Houen, G., 2018. Antibodies to a strain-specific citrullinated Epstein-Barr virus peptide diagnoses rheumatoid arthritis. Scientific Reports 8, 3684. https://doi.org/10.1038/s41598-018-22058-6

van Venrooij, W.J., van Beers, J.J.B.C., Pruijn, G.J.M., 2011. Anti-CCP antibodies: the past, the present and the future. Nat Rev Rheumatol 7, 391–398. https://doi.org/10.1038/nrrheum.2011.76

Vossenaar, E.R., Zendman, A.J.W., Van Venrooij, W.J., Pruijn, G.J.M., 2003. PAD, a growing family of citrullinating enzymes: Genes, features and involvement in disease. BioEssays 25, 1106–1118. https://doi.org/10.1002/bies.10357

Warren, T.K., Jordan, R., Lo, M.K., Ray, A.S., Mackman, R.L., Soloveva, V., Siegel, D., Perron, M., Bannister, R., Hui, H.C., Larson, N., Strickley, R., Wells, J., Stuthman, K.S., Van Tongeren, S.A., Garza, N.L., Donnelly, G., Shurtleff, A.C., Retterer, C.J., Gharaibeh, D., Zamani, R., Kenny, T., Eaton, B.P., Grimes, E., Welch, L.S., Gomba, L., Wilhelmsen, C.L., Nichols, D.K., Nuss, J.E., Nagle, E.R., Kugelman, J.R., Palacios, G., Doerffler, E., Neville, S., Carra, E., Clarke, M.O., Zhang, L., Lew, W., Ross, B., Wang, Q., Chun, K., Wolfe, L., Babusis, D., Park, Y., Stray, K.M., Trancheva, I., Feng, J.Y., Barauskas, O., Xu, Y., Wong, P., Braun, M.R., Flint, M., McMullan, L.K., Chen, S.S., Fearns, R., Swaminathan, S., Mayers, D.L., Spiropoulou, C.F., Lee, W.A., Nichol, S.T., Cihlar, T., Bavari, S., 2016. Therapeutic efficacy of the small molecule GS-5734 against Ebola virus in rhesus monkeys. Nature 531, 381–385. https://doi.org/10.1038/nature17180

Weiss, S.R., Navas-Martin, S., 2005. Coronavirus Pathogenesis and the Emerging Pathogen Severe Acute Respiratory Syndrome Coronavirus. MICROBIOLOGY AND MOLECULAR BIOLOGY REVIEWS 69, 635–664. https://doi.org/10.1128/MMBR.69.4.635-664.2005

Willis, V.C., Banda, N.K., Cordova, K.N., Chandra, P.E., Robinson, W.H., Cooper, D.C., Lugo, D., Mehta, G., Taylor, S., Tak, P.P., Prinjha, R.K., Lewis, H.D., Holers, V.M., 2017. Protein arginine deiminase 4 inhibition is sufficient for the amelioration of collagen-induced arthritis. Clin Exp Immunol 188, 263–274. https://doi.org/10.1111/cei.12932

Willis, V.C., Gizinski, A.M., Banda, N.K., Causey, C.P., Knuckley, B., Cordova, K.N., Luo, Y., Levitt, B., Glogowska, M., Chandra, P., Kulik, L., Robinson, W.H., Arend, W.P., Thompson, P.R., Holers, V.M., 2011. N-α-Benzoyl-N5-(2-Chloro-1-Iminoethyl)-l-Ornithine Amide, a Protein Arginine Deiminase Inhibitor, Reduces the Severity of Murine Collagen-Induced Arthritis. The Journal of Immunology 186, 4396–4404. https://doi.org/10.4049/jimmunol.1001620

Wing, P.A.C., Keeley, T.P., Zhuang, X., Lee, J.Y., Prange-Barczynska, M., Tsukuda, S., Morgan, S.B., Harding, A.C., Argles, I.L.A., Kurlekar, S., Noerenberg, M., Thompson, C.P., Huang, K.Y.A., Balfe, P., Watashi, K., Castello, A., Hinks, T.S.C., James, W., Ratcliffe, P.J., Davis, I., Hodson, E.J., Bishop, T., McKeating, J.A., 2021. Hypoxic and pharmacological activation of HIF inhibits SARS-CoV-2 infection of lung epithelial cells. Cell Reports 35, 109020. https://doi.org/10.1016/j.celrep.2021.109020

Witalisom, E., Thompson, R., Hofseth, L., 2002. Protein Arginine Deiminases and Associated Cirtullination. Anuario musical: Revista de musicolog{í}a del CSIC 16, 199–227.

Wu, F., Zhao, S., Yu, B., Chen, Y.M., Wang, W., Song, Z.G., Hu, Y., Tao, Z.W., Tian, J.H., Pei, Y.Y., Yuan, M.L., Zhang, Y.L., Dai, F.H., Liu, Y., Wang, Q.M., Zheng, J.J., Xu, L., Holmes, E.C., Zhang, Y.Z., 2020. A new coronavirus associated with human respiratory disease in China. Nature 579, 265–269. https://doi.org/10.1038/s41586-020-2008-3

Yang, L., Tan, D., Piao, H., 2016. Myelin Basic Protein Citrullination in Multiple Sclerosis: A Potential Therapeutic Target for the Pathology. Neurochemical Research 41, 1845–1856. https://doi.org/10.1007/s11064-016-1920-2

Yuzhalin, A.E., 2019. Citrullination in Cancer. Cancer Res 79, 1274–1284. https://doi.org/10.1158/0008-5472.CAN-18-2797

Zaki, A.M., van Boheemen, S., Bestebroer, T.M., Osterhaus, A.D.M.E., Fouchier, R.A.M., 2012. Isolation of a Novel Coronavirus from a Man with Pneumonia in Saudi Arabia. New England Journal of Medicine 367, 1814–1820. https://doi.org/10.1056/nejmoa1211721

Zhao, T., Pan, B., Alam, H.B., Liu, B., Bronson, R.T., Deng, Q., Wu, E., Li, Y., 2016. Protective effect of Cl-amidine against CLP-induced lethal septic shock in mice. Sci Rep 6, 36696. https://doi.org/10.1038/srep36696

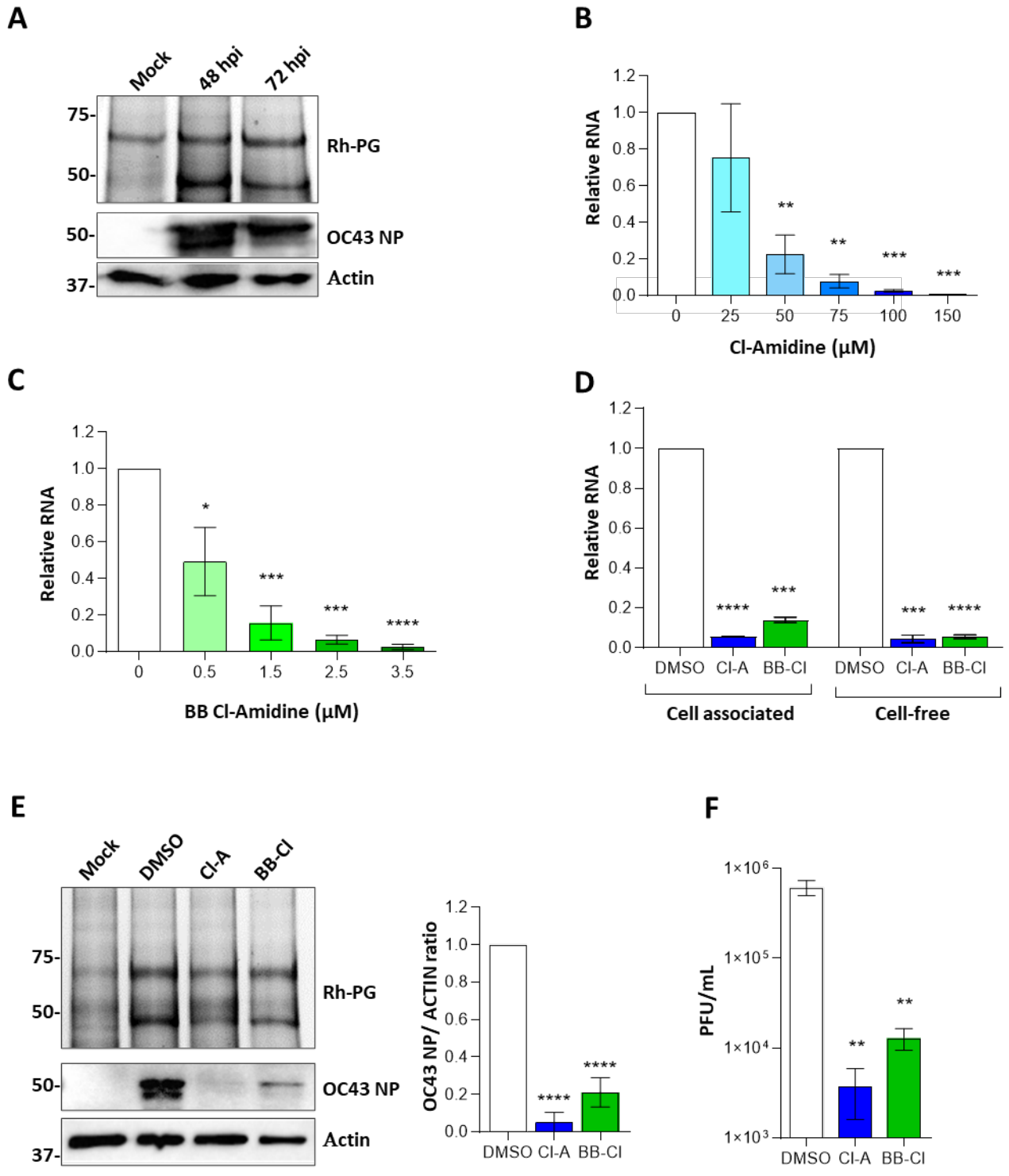


**Fig. 1. The pan-PAD inhibitors Cl-A and BB-Cl hamper HCoV-OC43 replication in MRC-5 cells.** (A) Protein lysates from MRC-5 cells infected with HCoV-OC43 (MOI 1) at 48 and 72 h post infection (hpi) or from uninfected control cells (Mock) were exposed to Rh-PG probe (top panel) and subjected to gel electrophoresis to detect citrullinated proteins. Viral protein expression (OC43 NP) and equal loading (actin) were assessed by Western blot analysis (bottom panels). One

representative gel of three independent experiments is shown. (B, C) Dose-response curves of the cell-permeable pan-PAD inhibitors Cl-A (A) and BB-Cl (B). MRC-5 cells were infected with HCoV-OC43 (MOI 0.1) and treated with increasing amounts of the drugs, which were given 1 h prior to virus adsorption and kept throughout the whole experiment. After 72 hpi, the viral load was determined by RT-PCR and expressed as percentage relative to the untreated control. Values are expressed as mean ± SEM of three independent experiments. (D) MRC-5 cells were pre-treated with Cl-A (100 μM) or BB-Cl (2.5 μM) for 1 h and then infected with HCoV-OC43 (MOI 0.1). After 72 hpi, viral replication was assessed by RT-PCR on cell-associated viral RNA, previously extracted from infected cells, or on the supernatants collected from infected cells. Values are expressed as mean ± SEM of three independent experiments. (E) MRC-5 cells were infected with HCoV-OC43 (MOI 0.1) and then treated with Cl-A (100 μM) or BB-Cl (2.5 μM) as described in B. Protein lysates were prepared at 48 hpi and exposed to Rh-PG probe (top panel). Viral protein expression (OC43 NP) and equal loading (actin) were assessed by Western blot analysis (one representative experiment out of three is reported, bottom panels) and quantified by densitometric analysis (right panel). (F) Viral productions were collected at 72 hpi and analyzed by plaque-forming assay. Values are expressed as mean ± SEM of three independent experiments. *P*-value < 0.05 (*), < 0.01 (**), < 0.001 (***) and < 0.0001 (****).

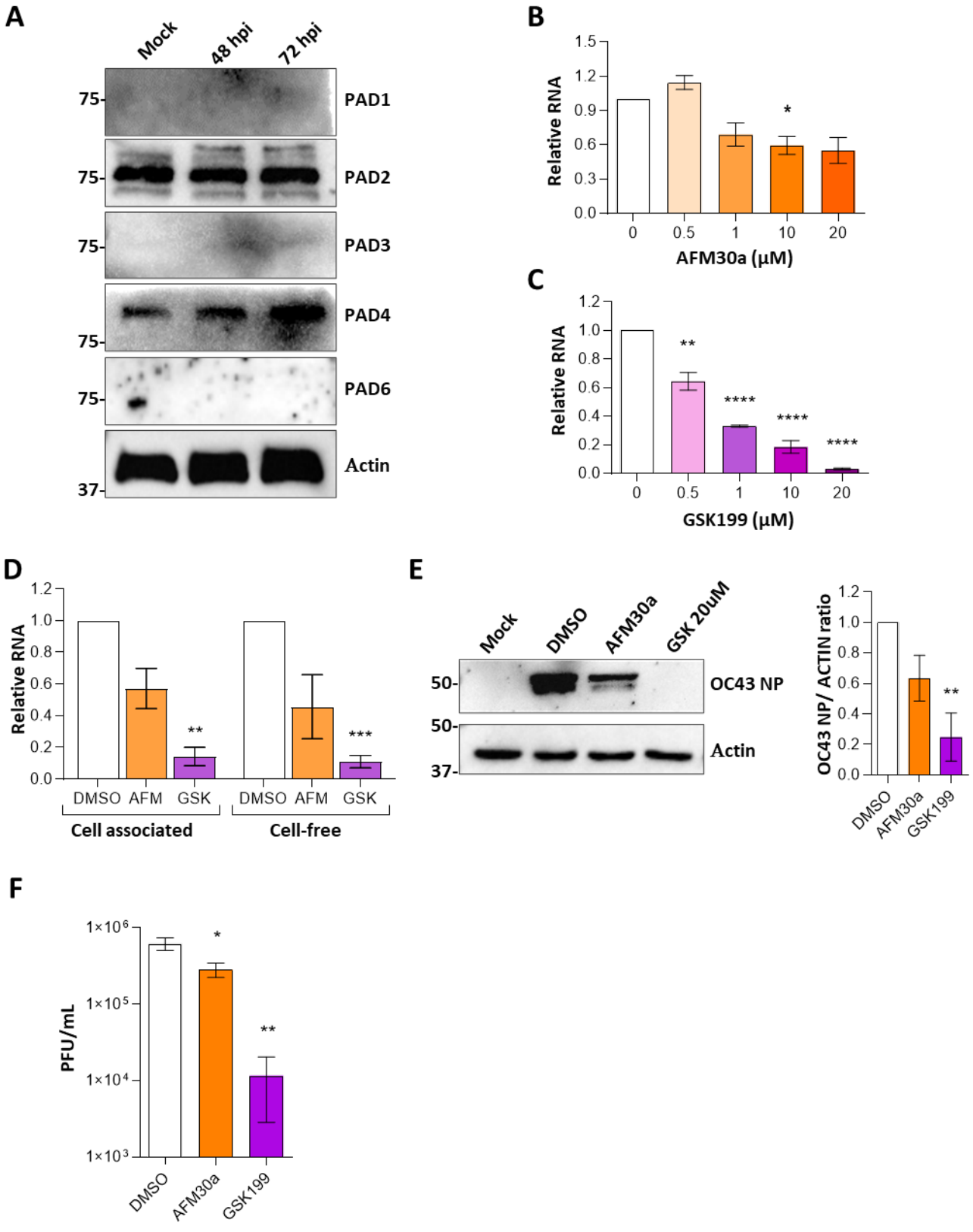


**Fig. 2. Effect of specific PAD2 and PAD4 inhibitors on HCoV-OC43 replication in MRC-5 cells.**

(A) Western blot analysis of protein lysates from uninfected (mock) or infected MRC-5 cells using antibodies against PAD1, PAD2, PAD3, PAD4, PAD6, or β-actin. The blot shown is representative

of three independent experiments. (B-C) Dose-response curves of the PAD2 (AFM30a) and PAD4 (GSK199) inhibitors. MRC-5s were infected with HCoV-OC43 (MOI 0.1) and then treated with increasing concentrations of the aforementioned drugs, as described in the legend to Fig 1. After 72 hpi, the viral load was determined by RT-PCR and expressed as a percentage relative to the untreated control. Values are expressed as mean ± SEM of three independent experiments. (D) MRC-5 cells were pre-treated with AFM30a (20 μM) or GSK199 (20 μM) for 1 h. Subsequently, cells were infected with HCoV-OC43 (MOI 0.1). The extent of HCoV-OC43 replication was then assessed by RT-PCR of viral RNA contained in cellular lysates (cell associated) or supernatants (cell-free) at 72 hpi. Values are expressed as mean ± SEM of three independent experiments. (E, F) MRC-5 cells were infected with HCoV-OC43 (MOI 0.1) and then treated with AFM30a or GSK199, as described in D. Protein lysates were prepared at 48 hpi and viral protein expression (OC43 NP) and equal loading (β-actin) were assessed by Western blot analysis (one representative experiment out of three is reported in E, left panel) and quantified by densitometric analysis (E, right panel). Viral productions were collected at 72 hpi and analyzed by plaque assay (F). Values are expressed as mean ± SEM of three independent experiments. *P*-value < 0.05 (*), < 0.01 (**), < 0.001 (***) and < 0.0001 (****).

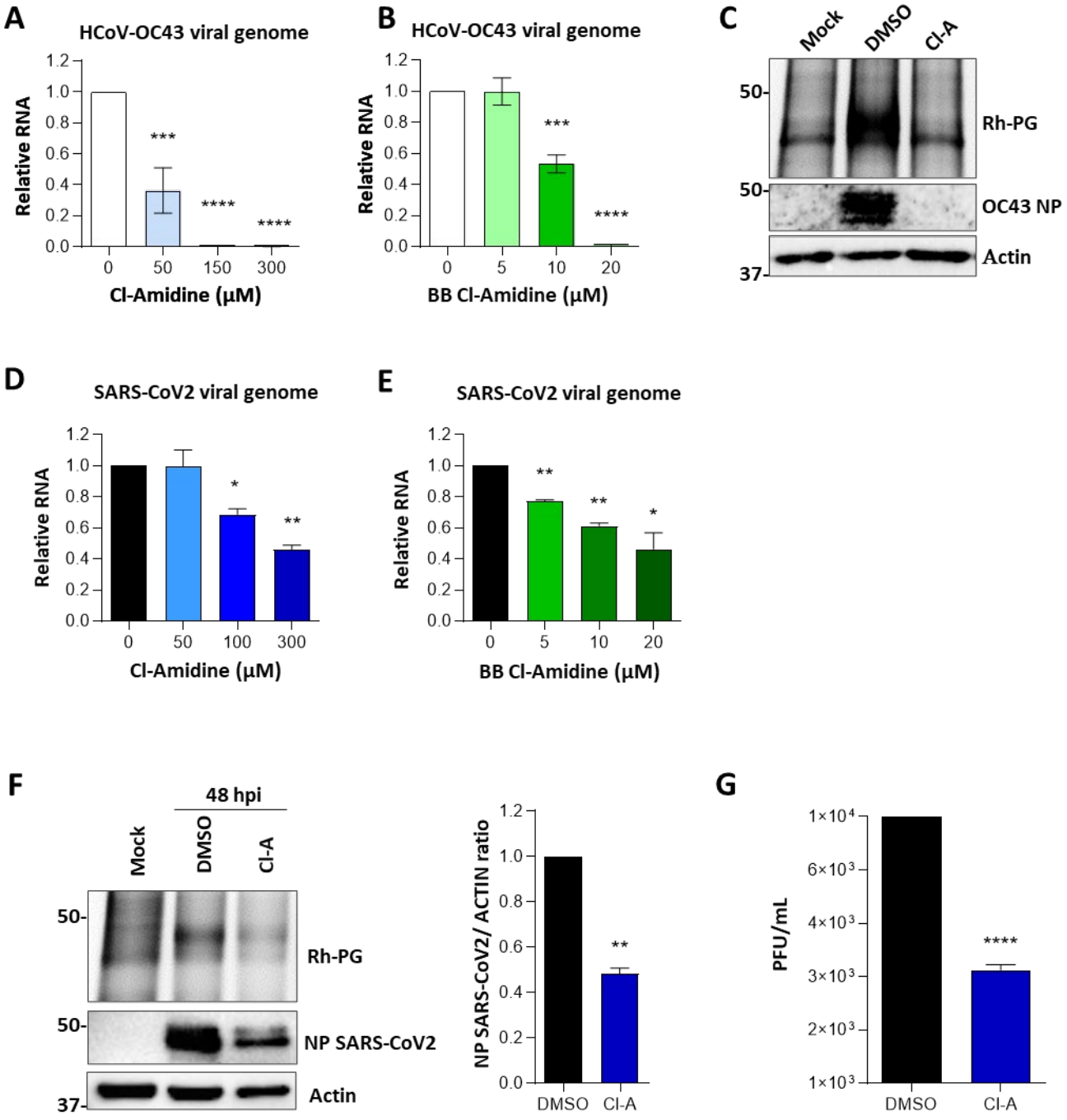


**Fig. 3. The pan-PAD inhibitors Cl-Amidine and BB-Cl-Amidine block β-coronavirus replication in Vero-E6 cells.** (A, B) Vero-E6 cells were infected with HCoV-OC43 (MOI 0.1) and then treated with increasing concentrations of Cl-A (A) or BB-Cl (B), which were given 1 h prior to virus adsorption and kept throughout the whole experiment. After 72 hpi, the viral load was determined by RT-PCR and expressed as a percentage relative to the untreated control. Values are expressed as mean ± SEM of three independent experiments. (C) Vero-E6 cells were treated with Cl-

A (300 μM) or with equal volumes of DMSO 1 h before infection and for the entire duration of the infection, and infected with HCoV-OC43 at a MOI of 1. Protein lysates were prepared at 48 hpi and subjected to Rh-PG (top panel) and Western blot (bottom panels) analyses. One representative blot is shown of three independent experiments. (D, E) Vero-E6 cells were infected with SARS-CoV-2 (MOI 0.1) and then treated as described in A. After 72 hpi, the viral load was determined by RT-PCR and expressed as the percentage relative to untreated control. Values are expressed as mean ± SEM of three independent experiments. (F) Vero-E6 cells were infected with SARS-CoV-2 (MOI 1) and then treated as described in C. Protein lysates were prepared at 48 hpi and subjected to Rh-PG (top panel) and Western blot (bottom panels) analyses. The blot shown is representative of three independent experiments. (G) Vero-E6 cells were infected with SARS-CoV-2 (MOI 0.1) and then treated as described in C. Viral productions were collected at 72 hpi and analyzed by plaque assay. Values are expressed as mean ± SEM of three independent experiments. *P*-value < 0.05 (*), < 0.01 (**), < 0.001 (***) and < 0.0001 (****).

**Supplementary**

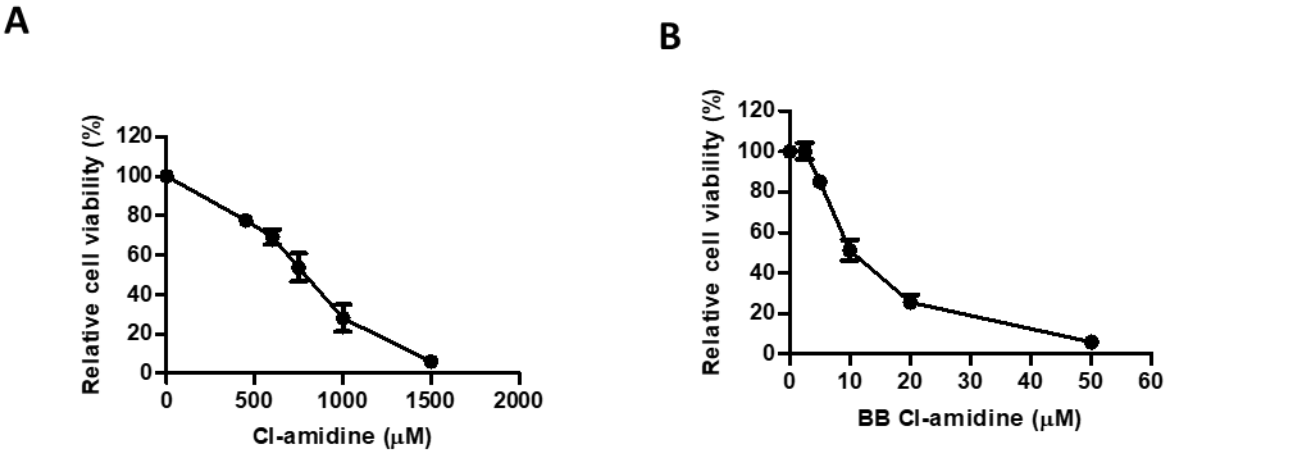


**Figure S1**

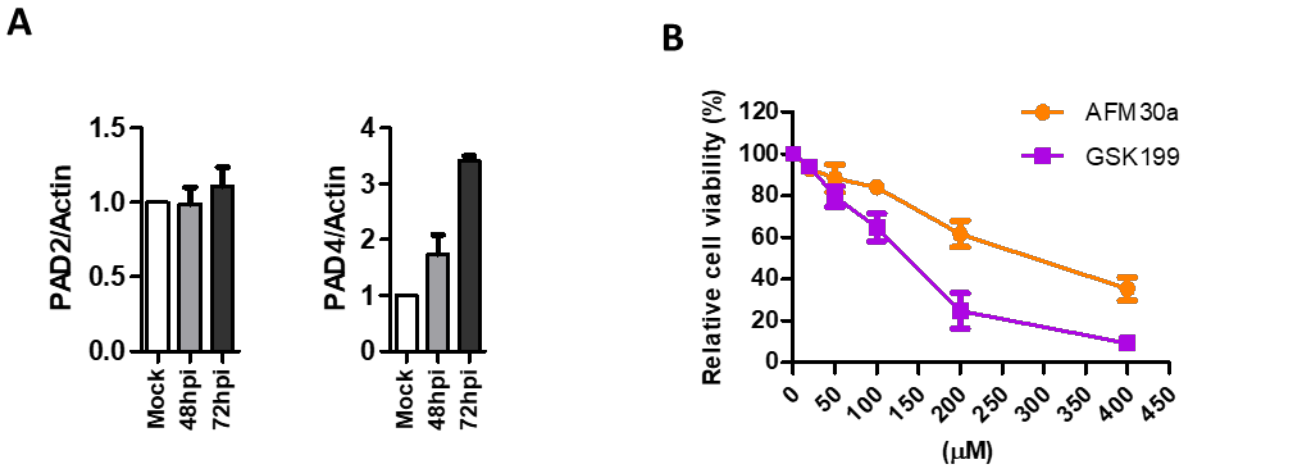


**Figure S2**

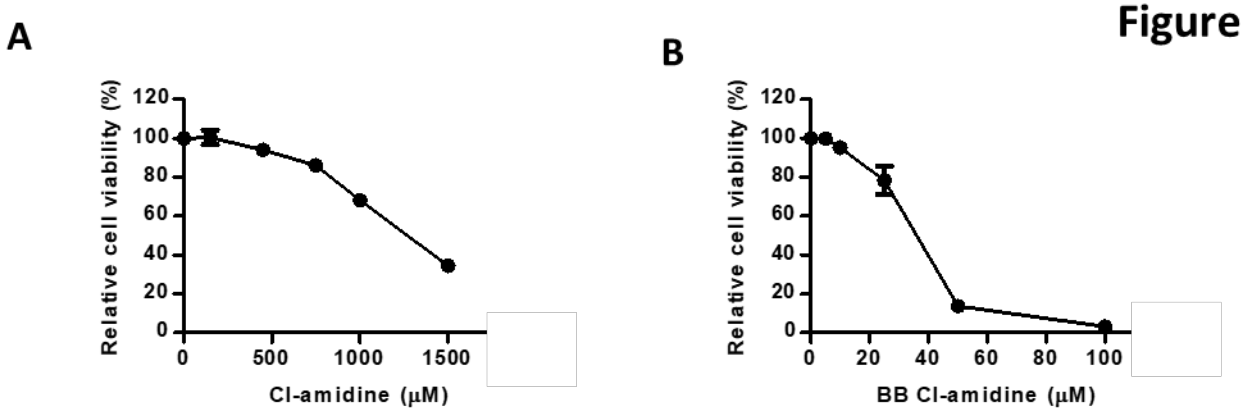


**Figure S3**

**Fig. S1. (**A, B) MTT assay. Uninfected MRC-5 cells were treated with the indicated concentrations of Cl-amidine and BB-Cl-amidine or DMSO alone for 72 h and subjected to MTT assay. Values are expressed as mean ± SEM of three independent experiments.

**Fig. S2.** (A, B) Densitometric analysis. **C)** MTT assay. Uninfected MRC-5 cells were treated MRC-5 cells were treated with the indicated concentrations of AFM30a or GSK199 or DMSO alone for 72 h. Values are expressed as mean ± SEM of three independent experiments.

**Fig. S3** (A, B) The MTT assay was performed in uninfected Vero-E6 cells using different concentrations of drugs. MRC-5 cells were treated with different concentrations of Cl-A (A) or BB-Cl (B) for 72 h. Values are expressed as mean ± SEM of three independent experiments.

**Table 1**

$CC_{50}$, $IC_{50}$, and SI of PAD inhibitors against beta-CoVs

| cell/virus | compound | [µM] | | |
|---|---|---|---|---|
| | | IC50 | CC50 | SI |
| MRC-5/OC43 | Cl-Amidine | 34.80 | 949.14 | 27.30 |
| | BB-Cl-Amidine | 0.53 | 10.12 | 18.62 |
| | GSK199 | 0.60 | 133.08 | 224.94 |
| | AFM30a | > 20 | 320.92 | > 16 |
| Vero-E6/OC43 | Cl-Amidine | 44.15 | > 1000 | > 22 |
| | BB-Cl-Amidine | 10.68 | 33.06 | 3.10 |
| Vero-E6/SARS-CoV-2 | Cl-Amidine | 95.17 | > 1000 | > 10 |
| | BB-Cl-Amidine | 17.78 | 33.06 | 1.86 |